Conformational States of the Bacteriophage P22 Capsid Subunit in Relation to Self-Assembly†

Peter E. Prevelige, Jr.,‡ Dennis Thomas,‡ Jonathan King,‡ Stacy A. Towse,§ and George J. Thomas, Jr.*,§
Division of Cell Biology and Biophysics, School of Basic Life Sciences, University of Missouri—Kansas City, Kansas City, Missouri 64110, and Department of Biology, Massachusetts Institute of Technology, Cambridge, Massachusetts 02139
Received December 26, 1989; Revised Manuscript Received March 6, 1990

ABSTRACT: The formation of closed icosahedral capsids from a single species of coat protein subunit requires that the subunits assume different conformations at different lattice positions. In the double-stranded DNA bacteriophage P22, formation of correctly dimensioned capsids is mediated by interaction between coat protein subunits and scaffolding protein. Raman spectroscopy has been employed to compare the conformations of coat protein subunits which have been polymerized to form capsids in the presence and absence of the scaffolding protein. Coat protein subunits polymerized into closed procapsid shells (PS) in the presence of scaffolding protein display a Raman spectrum characterized by a broad amide I band centered at 1665 cm^{-1} with a discernible shoulder near 1653 cm^{-1}, and a broad amide III profile centered at 1238 cm^{-1} but asymmetrically skewed to higher frequency. These spectral features indicate that the protein conformation in procapsid shells is rich in β-sheet secondary structure but contains also a significant distribution of α-helix. When biologically active, purified subunits assemble in the absence of scaffolding protein, they form polydisperse multimers lacking the proper dimensions of procapsid closed shells. We designate these multimers as "associated subunits" (AS). The Raman spectrum of associated subunits indicates a narrower distribution of secondary structure. The associated subunits are characterized by a sharper and more intense Raman amide I band at 1666 cm^{-1}, with no prominent amide I shoulder of lower frequency. An analogous narrowing of the Raman amide III profile is also observed for AS particles, with an accompanying shift of the amide III band center to 1235 cm^{-1}. These findings indicate a clear-cut conversion of α-helical secondary structure in subunits of PS particles to the β-sheet conformation in subunits of AS particles. Band intensity analysis shows that this conformation switch involves 4.5% (±0.4%) of peptide residue conformational states. Specifically, Raman difference spectroscopy applied in combination with signal averaging to probe small changes in protein secondary structure reveals that the converted α-helical domain of PS constitutes 2.3% (±0.2%) of the polypeptide chain, or 10 (±1) of 430 residues in the gp5 subunit. These residues adopt the β-sheet structure in AS particles. The PS → AS difference is accompanied by pronounced changes in Raman bands associated with specific amino acid side chains. In particular, the hydrogen bonding states of tyrosine and tryptophan residues are altered significantly by the PS → AS transition, as are the conformations of aliphatic side chains. The changes observed in the Raman bands of specific amino acid residues are generally indicative of a greater variety of side chain environments for the AS state, including more solvent exposure of tyrosine and tryptophan residues. The data are thus compatible with a more β-rich secondary structure and less compact tertiary structure for the associated subunits.

The capsids of spherical viruses display an overall icosahedral symmetry though they contain hundreds of protein subunits. Since the surface of an icosahedron can accommodate only 60 identical subunits, locating hundreds requires a sophisticated packing scheme. The concept of quasi-equivalence as originally proposed by Caspar and Klug suggests that in order to accommodate more than 60 subunits on the surface of an icosahedron the faces are subtriangulated (Caspar & Klug, 1962). Since subtriangulation necessarily produces inequivalencies in subunit bonding contacts, Caspar and Klug originally proposed that these inequivalencies could be accommodated through minor elastic distortions in the subunit bonding contacts. The energy required for deforming the bonding contacts would be supplied by the energy of shell closure. However, with the availability of high-resolution structures for a number of viral particles, it has become apparent that quasi-equivalence is often violated (Rayment et al., 1982; Rossman, 1984). The subunits occupying different positions in a mature viral particle exist in different and well-defined conformations. Building a closed viral capsid therefore requires that protein subunits in distinct conformations occupy their appropriate locations within the growing shell. Accurate switching between the possible subunit conformations in the context of the growing shell is presumably required in order to build properly dimensioned closed capsid shells. Switching of a protein subunit between unassociable and associable forms at the growing edge of a structure has been termed autosteric switching (Caspar, 1980). It is likely that selection of the proper subunit conformation is coupled to this process.

The coat protein subunit of the *Salmonella* phage P22 is capable of existing in a number of different assembly states in vivo. The subunit, which is the product of viral gene 5 (gp5), does not spontaneously assemble into capsids, but first requires the formation of a metastable precursor particle called the procapsid (King et al., 1973). Procapsid assembly requires the copolymerization of 420 molecules of coat protein and 240 molecules of scaffolding protein (gp8). In this procapsid, the coat protein forms a topologically closed exterior shell, with a lattice very similar to that of the mature capsid, and encloses an inner shell of scaffolding protein (Earnshaw et al., 1976;

† Studies of Virus Structure by Raman Spectroscopy, Part XXIX. Supported by NIH Grants AI11855 (G.J.T.) and GM17980 (J.K.).
* To whom correspondence should be addressed.
‡ Massachusetts Institute of Technology.
§ University of Missouri—Kansas City.

0006-2960/90/0429-5626$02.50/0

Casjens, 1979). The transformation from the metastable procapsid to the mature capsid requires packaging of the genomic DNA, and concomitant with DNA packaging, the radius of the shell increases by approximately 10%, probably by a hinge-bending movement of a coat protein subunit domain (Casjens, 1979). As DNA is packaged, the scaffolding protein exits and is free to participate in further rounds of assembly (King & Casjens, 1974). The DNA is packaged through a unique portal vertex consisting of a dodecamer of the product of gene 1 (Bazinet & King, 1985; Bazinet et al., 1988).

The formation of a stable capsid requires additionally that protein products of genes 4, 10, and 26 interact with the newly filled capsid, presumably to close the portal. In mutants which do not produce any one of these proteins, the newly packaged DNA leaks out, leaving empty but stable coat protein shells (Strauss & King, 1984).

In vivo in the absence of scaffolding protein, the coat protein does not polymerize until a high intracellular coat protein concentration is reached. This scaffold-free polymerization process produces aberrant structures, consisting of improperly dimensioned shells and spiral assemblies. These structures which display improper radii of curvature likely arise from incorrect relative positioning of 5-fold and 6-fold vertices in the growing structure (Earnshaw & King, 1978). Similar results have been obtained in vitro using purified coat protein subunits (Fuller & King, 1982).

We have recently described an in vitro system in which purified coat protein subunits display the assembly properties observed in vivo (Prevelige et al., 1988). In order to detect and charaterize specific conformational states at the molecular level, we have examined the coat protein subunit assemblies by Raman spectroscopy. The feasibility of employing Raman spectroscopy as a probe of structure of P22 proteins, including gp5 and gp8, was demonstrated in an earlier study of capsids and procapsids (Thomas et al., 1982). Instrumentation and methods employed in the earlier study did not permit extensive signal averaging of the collected data to reduce transient noise, and did not implement solvent correction of the solution spectra with the precision afforded by digital difference procedures. In effect, conformational differences involving less than 10% of the protein secondary structure could not be measured definitively. The present study, utilizing techniques of higher sensitivity, allows the detection of conformational differences involving as few as 2% of the peptide residues per subunit. The results obtained in this work demonstrate that the conformation of coat protein subunits in topologically closed procapsid shells (PS) assembled under the control of scaffolding protein is different than the conformation of the same associated subunits (AS) self-assembled in the absence of scaffolding protein.

Experimental Procedures

Preparation and Purification of Phage P22 Proteins

Strains. All bacterial and phage strains were derived or constructed from parent strains in the collections of D. Botstein or J. King. Bacterial strains are derivatives of *Salmonella typhimurium* LT2. The suppressor minus host DB7136 [leu A414(am), his C525(am)] and its su$^+$ derivative DB7155 [leu A414(am) his C525(am) supE20] have been described (Winston et al., 1979). The phage employed in the production of procapsid proteins was 2$^-$amH200/13$^-$amH1010c1-7. This phage carries an amber mutation in gene 2 preventing DNA packaging, and hence yielding procapsids as a final product. It also carries the c1-7 allele to ensure entry in the lytic cycle, and an amber mutation in gene 13 which results in continuation of procapsid production past the normal lysis time.

Media and Chemicals. LB broth, LB bottom agar, and soft agar were used for routine propagation of host cells and phage (Chan & Botstein, 1972). Superbroth (Fuller & King, 1981) was used for the growth of cells from which procapsids were purified. Buffer B is defined as 50 mM Tris-HCl, 25 mM NaCl, and 2 mM EDTA, pH 7.6. Other chemicals and sources are as defined in Fuller and King (1981). All dialysis tubing employed was Spectrapor (Spectrum Medical Industries, Los Angeles, CA), prepared as described (Prevelige & Fasman, 1987).

Procapsid Purification. To prepare large quantities of procapsids, 12 L of superbroth was inoculated with the nonpermissive host strain DB7136 in a fermenter and grown to a density of 2×10^8 cells/mL at 35 °C. The cells were infected with 2$^-$amH200/13$^-$amH101/c1-7 phage at a multiplicity of 5 phage/cell. The cells were harvested 3.5 h after infection. Antifoam was added as necessary during the infection. The cells were rapidly chilled and pelleted by centrifugation at 3000*g* for 5 min. The supernatant was discarded, and the pelleted cells were resuspended in 120 mL of lysis buffer (50 mM Tris-HCl/20 mM $MgCl_2$, pH 7.6), rapidly frozen in liquid N_2, and stored at −20 °C. The frozen cells were thawed at 37 °C in the presence of 1 mM PMSF and saturating chloroform. This freeze/thawing cycle was repeated 3 times. The lysed cells were incubated with 100 μg/mL DNase at 37 °C for 30 min. Following the DNase treatment, cell debris was removed by centrifugation at 17000*g* for 20 min, and the supernatant, containing the procapsids, was reserved. The pellets were resuspended in 60 mL of 50 mM Tris-HCl/100 mM EDTA, pH 7.6, and the centrifugation was repeated to recover any procapsids trapped in the pellet. The supernatants from both steps were pooled and incubated with 50 μg/mL RNase at 30 °C for 30 min. The RNase-treated solution was centrifuged at 17000*g* for 20 min and the supernatant reserved. To harvest the procapsids, the supernatant was centrifuged at 35 000 rpm in a Beckman LM-8 ultracentrifuge (Ti-45 rotor) for 45 min at 4 °C. The pellets were resuspended in buffer B and centrifuged at 17000*g* for 20 min to remove any insoluble material. The crude procapsids were applied to an 80-mL S-1000 column in 8 mL of buffer B. The column was developed with buffer B at 4 °C, at a flow rate of 20 mL/h, with 5-mL fractions collected. The procapsid-containing peak was located by a combination of absorbance measurements and SDS–PAGE. The procapsid-containing fractions were pooled, concentrated, and washed by ultracentrifugation.

Scaffolding Protein Extraction. The scaffolding protein was extracted from the procapsids by addition of 1 M Gdn-HCl in buffer B to a final concentration of 0.5 M followed by centrifugation in a Ti-45 rotor at 35 000 rpm for 45 min. The supernatant contained the scaffolding protein, and the pellet contained coat protein shells. The extraction process was repeated until the absorbance in the supernatant fraction was minimal. Typically, three extractions were performed with an extraction volume of 135 mL.

Purification of Shells of Coat Protein. Shells consisting of coat protein were purified by chromatography on a Bio-Gel A-0.5m size-exclusion column in 0.5 M Gdn-HCl. The shell-containing fractions were pooled and concentrated to 40 mg/mL by centrifugation followed by resuspension in buffer B. In order to remove any residual scaffolding protein, as well as the minor proteins gp1, gp16, and gp20, the shells were treated with 0.8% SDS. It has been shown that this procedure effectively removes all proteins other than the coat proten from the shell (Casjens & King, 1974). Since this preparative procedure does not effectively discriminate against stable, high

molecular weight species such as residual input phage, the shells were further purified by centrifugation on a CsCl step gradient. Step gradients were constructed out of 4 mL each of 1.2, 1.3, 1.4, and 1.5 g/cm^3 CsCl in 50 mM Tris/20 mM $MgCl_2$, pH 7.5. One milliliter of coat protein shells was loaded on each gradient, and the gradients were centrifuged in an SW27.1 rotor at 24000 rpm for 4 h at 4 °C. The coat protein shells banded between 1.2 and 1.3 g/cm^3, and contaminating phage between 1.4 and 1.5 g/cm^3. The bands corresponding to shells were removed from the gradient, diluted 3-fold with buffer B, and concentrated by centrifugation in a Ti-45 rotor at 24000 rpm for 45 min at 4 °C. The samples were then dialyzed against buffer B overnight. The shells were divided into two equal volumes. One was made 3 M in Gdn-HCl at a final concentration of 1.2 mg/mL. This material was dialyzed out of Gdn-HCl in Spectrapor 3 dialysis tubing at 4 °C. We have previously demonstrated that this protocol results in the formation of monomeric coat protein capable of assembling into procapsid-like particles in the presence of scaffolding protein. The dialyzed (monomeric) coat protein was assayed for its ability to form procapsids in the presence of scaffolding protein. The coat protein monomers and the remaining shells were each dialyzed against 10 mM Tris, 25 mM NaCl, and 2 mM EDTA, pH 7.5, at room temperature and concentrated by using an Amicon stirred cell equipped with a PM-30 membrane under 20 psi N_2 at room temperature. These stock solutions were further prepared for Raman spectroscopic analysis, as indicated under Raman Instrumentation and Sample Handling Procedures.

Sucrose Gradient Centrifugation. Sucrose gradient centrifugation was performed essentially as previously described (Prevelige et al., 1988). Samples of 100 μL were mixed with 5 μL of BSA at 10 mg/mL and layered on 5-mL 5–20% sucrose gradients. Centrifugation was at 35000 rpm for 35 min at 20 °C. Gradients were fractionated into constant-volume fractions, and the protein content of each fraction was analyzed by SDS–PAGE.

Electron Microscopy. Negative staining was done by the method of Huxley and Zubay (1960) using 2% (w/v) uranyl acetate.

Raman Instrumentation and Sample Handling Procedures

The stock solution containing procapsid shells (PS) at 20 μg/μL, prepared as indicated above, was concentrated further for Raman spectroscopy according to the following procedure. The PS solution was introduced into a Centricon microconcentrator (Amicon Corp.) and was subjected to low-speed centrifugal sieving through a membrane with a molecular weight cutoff of 10K, achieving a 2-fold increase in PS concentration. Aliquots (≈10 μL) of this material, in pH 7.1 ± 0.1 buffer (10 mM Tris, 25 mM NaCl, and 2 mM EDTA), were transferred to Kimax 34507 glass capillary tubes and sealed. The stock solution of associated subunits (AS) in the same buffer was subjected to a low-speed spin to pellet AS particles at the same approximate concentration (≈40 μg/μL) as for PS, and 10-μL aliquots of the pelleted AS material were also sealed in glass capillaries. The sealed capillaries were mounted in a precision thermostat (20 °C) for spectroscopic analysis (Thomas & Barylski, 1970). Other details of sample handling for Raman spectroscopy of P22 proteins have been described (Thomas et al., 1982; Sargent et al., 1988).

Raman spectra were excited with the 514.5-nm line from an argon ion laser (Coherent Innova 70-2) using approximately 300 mW of power at the sample. Raman scattering at 90° to the incident laser beam was collected and analyzed with a Spex Ramalog V/VI spectrophotometer (Li et al., 1981), operating under the control of an IBM-PC. Programs for instrument control and data collection were developed in our laboratory using the ASYST language (Asyst Software Technologies). A detailed description of this software implementation will be given elsewhere (B. Prescott and G. J. Thomas, Jr., unpublished results). Data were collected with a spectral slit width of 8 cm^{-1}, at increments of 1 cm^{-1} in the region 500–1750 cm^{-1}, and with an integration time of 1.5 s. Survey spectra of both PS and AS were collected in this spectral range, and the Raman intensities from nine consecutive scans were averaged for presentation below. More extensive signal averaging, up to 40 scans, was carried out for narrower spectral intervals containing the conformation-sensitive aromatic ring (750–900 cm^{-1} interval), amide I (1500–1725 cm^{-1}), and amide III bands (1180–1380 cm^{-1}).

The Raman intensity data were corrected for scattering by the solvent and buffer, and for the gently sloping background characteristic of aqueous solution spectra of proteins. The scattering background was found to improve significantly for AS samples which had been allowed to equilibrate in the cold for long periods (up to several days) following transfer from the centrifuge tube to the Raman capillary cells. This effect was reproducible from one sample preparation to another, and is attributed to improvement in the optical homogeneity of the sample following transfer. Nonetheless, AS samples examined at different times during the equilibration period always yielded the same Raman spectrum.

Signal averaging, base-line corrections, spectral subtraction, and related data manipulations were performed through ASYST routines. Computation of Raman difference spectra in the amide I and amide III intervals for semiquantitative analysis of the amide band intensity changes accompanying the PS → AS transition was accomplished by normalization of the Raman amplitudes in the two samples so as to conserve the total integrated amide band intensity. Deconvolution procedures were carried out on an IBM microcomputer using software described previously (Thomas & Agard, 1984).

Since efficient in vitro association of subunits requires heating the Gdn-HCl-treated samples to 65 °C for up to 1 h (Prevelige et al., 1988), we monitored the Raman spectra of both AS and PS preparations as a function of heat treatment. The procapsid shells appear to be thermostable to 65 °C for short periods (less than 1 h), as judged by the invariance of the Raman spectrum. More prolonged heating leads to very small changes in the Raman spectrum, suggesting only minor structural changes in comparison with those reported below, possibly resulting from partial denaturation of the native subunit structure. AS particles, as expected, displayed a Raman spectrum that was completely invariant to 65 °C heat treatment, once the subunit association process was completed.

RESULTS

Description of Procapsid Shells. The procapsid shells employed in this study arise from extraction of the scaffolding protein from procapsids formed in vivo. The phage assembly process was stopped by using a mutant which prevents the packaging of DNA. The infected host cells accumulate procapsids, the double-shelled precursor particles with scaffolding protein molecules (gp8) composing the interior shell and capsid protein molecules (gp5) forming the exterior coat. The scaffolding protein is removed from the procapsid by treatment with 0.5 M Gdn-HCl. This extracts the scaffolding protein while leaving the shell of coat protein intact. These closed shells, herein called procapsid shells, were further dissociated with 3 M Gdn-HCl in order to obtain coat protein subunits

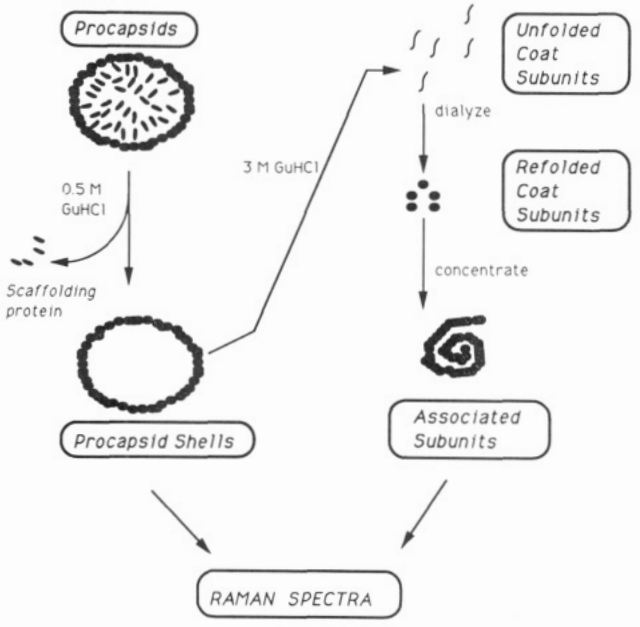

FIGURE 1: Flow chart illustrating preparation of procapsid shells and associated subunits for Raman spectroscopy. Procapsids isolated from phage-infected cells were treated with 0.5 M Gdn-HCl to remove scaffolding protein and to generate intact empty shells of coat protein, termed procapsid shells (left). The procapsid shells were dissociated in 3 M Gdn-HCl, yielding unfolded subunits, which were refolded and reassociated in solution to produce associated subunits (right).

(Figure 1). Treatment with 3 M Gdn-HCl results in unfolding of the coat protein subunits.

Refolding of Coat Protein Subunits. The purified coat protein subunits were refolded by dialysis at 4 °C out of Gdn-HCl at 1 mg/mL. This results in the production of biologically active monomeric coat protein (Prevelige et al., 1988). The coat protein was biologically active as witnessed by its ability to form procapsids upon addition of scaffolding protein. Upon further dialysis at room temperature, the sample became visibly turbid, indicating the formation of large aggregates. This coat protein was concentrated by ultrafiltration at room temperature under 20 psi N_2. The concentrated coat protein was analyzed by sucrose gradient centrifugation and electron microscopy.

The distribution of the coat protein across the sucrose gradient was analyzed by SDS gel electrophoresis (Figure 2). The coat protein was polydisperse; there is residual monomer present which we estimate to be about 7% of the total mass. There was a rapidly sedimenting peak of coat protein about halfway down the gradient. This position corresponds to the sedimentation of apparently closed shells and constitutes about 50% of the protein by weight. Electron microscopy confirms that the material in the peak position was rich in particles which, though apparently closed, lacked the uniform dimensions of procapsid shells. These improperly dimensioned shells are thus the major constituent in the polydisperse AS particles.

Reactivity of Cysteine Residues. The coat protein subunit contains a single cysteine (Cys) residue (S. Casjens, unpublished results), which is accessible to Ellman's reagent in the gp5 monomeric state. In shells and associated subunits, the Cys residue is no longer accessible. Dissociation of the AS particles with 3 M Gdn-HCl results in Cys residues again becoming accessible (P. Prevelige, G. J. Thomas, Jr., and J. King, unpublished results). We have used the accessibility of the subunit Cys residue to get an estimate of the residual monomer in the sample. On the basis of the Ellman's reagent assay of AS particles, we estimate that less than 5% of the AS sample consists of gp5 monomers.

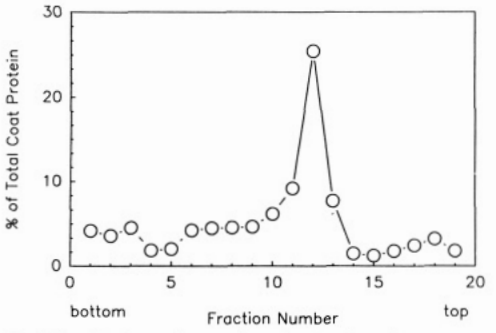

FIGURE 2: Distribution of associated subunits of coat protein in a 5–20% sucrose gradient. Approximately 150 μL of associated subunits was mixed with 5 μL of BSA at 10 mg/mL and applied to the top of a 5-mL 5–20% sucrose gradient. The gradient was centrifuged in an SW-50.1 rotor for 35 min at 35 000 rpm. The gradient was fractionated into 20 fractions of equal volume, and the protein distribution was analyzed by quantitative SDS gel electrophoresis.

Raman Spectroscopy. In our initial Raman study of P22 capsid and procapsid proteins (Thomas et al., 1982), extensive signal averaging of the data and solvent correction by digital difference methods were not possible. The limited sensitivity of the previous methods did not permit the discrimination of conformational differences affecting less than about 10% of subunit peptide residues in any one of the phage structural proteins. Though sufficient to distinguish the highly α-helical structure of the scaffolding protein from the more β-rich structures of the capsid and tailspike proteins, the earlier procedures did not permit the detection of conformational switching within any structural protein or among morphologically different particles (Thomas et al., 1982). Improved data collection and signal averaging methods now permit a greater than 5-fold increase in sensitivity over the previous technology. This advantage is exploited here in the comparison of Raman spectra of procapsid shell and associated subunit states of the P22 capsid protein.

Figure 3 shows the region 500–1725 cm^{-1} of the Raman spectra of procapsid shells (PS, bottom trace) and associated subunits (AS, top trace), prepared as described above. These two samples, both of which consist exclusively of the major coat protein (gp5) of P22, and both of which are dissolved at the same nominal subunit concentration in the same aqueous buffer, exhibit reproducible differences in a number of key conformation-sensitive Raman bands. The Raman bands of principal interest are labeled in Figure 3 (as referenced in the legend) to indicate their vibrational frequencies in cm^{-1} units and their residue assignments.

Figure 4 shows electron micrographs obtained from the same PS and AS specimens which have yielded the Raman spectra of Figure 3. These micrographs are typical of those obtained prior to laser Raman excitation of the identical samples, which confirms that the morphological states of the PS and AS particles are not altered by laser irradiation. Thus, the PS particles which yielded the lower spectrum of Figure 3 consist substantially of nativelike, empty capsids (Figure 4A). The AS particles which yielded the upper spectrum of Figure 3 consist of a variety of aggregated forms of gp5 (Figure 4B). None of the AS particles is a properly dimensioned closed shell, and all are morphologically distinct from and unable to assemble into the authentic shells. The Raman data shown here for PS particles are consistent with those reported in the previous preliminary study (Thomas et al., 1982). The Raman spectrum of the AS particles has not been studied previously.

(*a*) *Raman Amide Bands and Subunit Secondary Structure.* Raman spectra of significantly improved signal-to-noise quality were obtained for PS and AS particles by repetitive signal

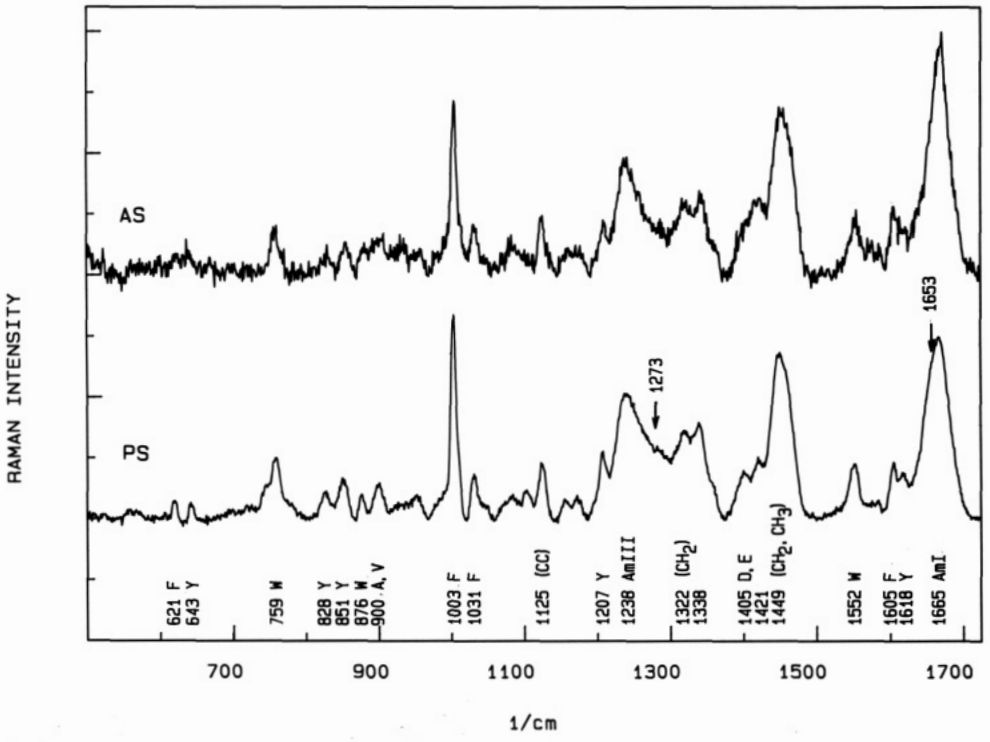

FIGURE 3: Survey Raman spectra in the region 500–1725 cm^{-1} of bacteriophage P22 procapsid shells (PS, bottom trace) and associated subunits (AS, top trace) obtained at 20 °C and with a spectral resolution of 8 cm^{-1}. The data have been corrected for background and for Raman scattering of the buffer (10 mM Tris, 25 mM NaCl, and 2 mM EDTA, pH 7.1). Labels indicate Raman frequencies in cm^{-1} units and probable assignments using one-letter abbreviations for the amino acids and standard nomenclature for chemical subgroups. Arrows indicate the location of amide I and amide III shoulders (α-helix) present in PS but not in AS. High-quality spectral traces from the amide I and amide III intervals, obtained by extensive signal averaging to reduce noise and illustrating the significant conformational change between PS and AS, are shown respectively in Figures 5 and 6.

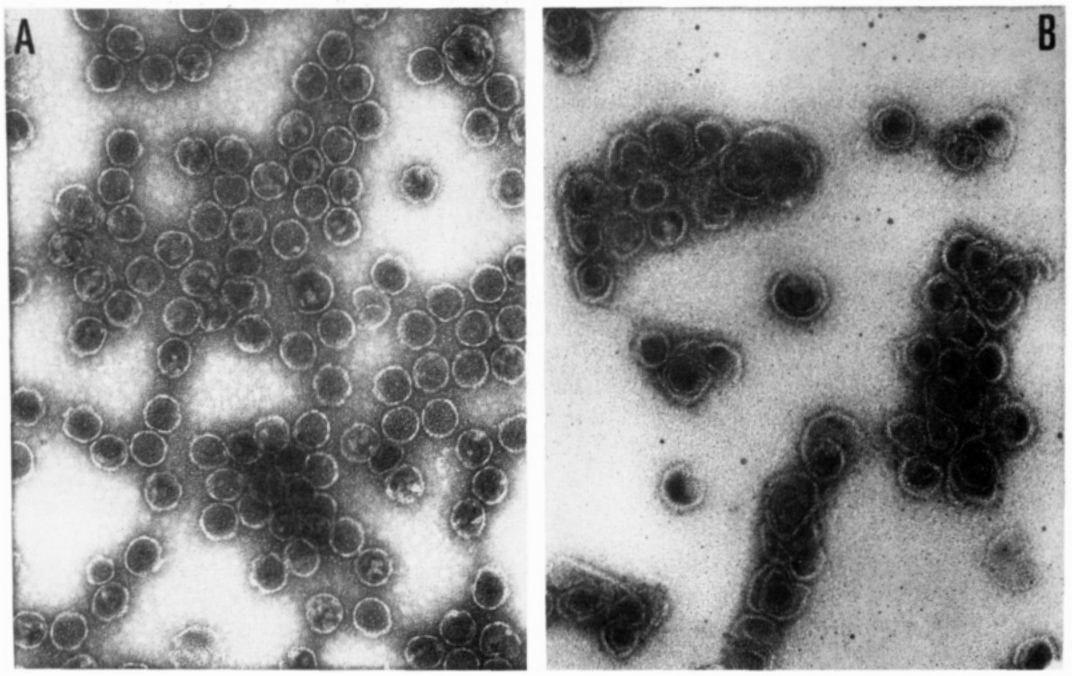

FIGURE 4: Electron micrographs of associated subunits (B) and procapsid shells (A) which yield the spectra of Figure 3. Samples were negatively stained with 2% (w/v) uranyl acetate.

averaging in the amide I (Figure 5) and amide III (Figure 6) regions. Included in each figure is the corresponding difference spectrum (AS minus PS). The frequencies of the difference Raman amide bands are labeled in the amplified traces of Figures 5 and 6. The data demonstrate a clear-cut shift of Raman amide I intensity from 1653 cm^{-1} (α-helix) in PS particles to 1665 cm^{-1} (β-sheet) in AS particles (Figure 5) and a concomitant shift of Raman amide III intensity from ca. 1273 cm^{-1} (α-helix) in PS to ca. 1238 cm^{-1} (β-sheet) in AS (Figure 6). The basis for the assignment of peaks and troughs in the difference spectra to specific secondary structure types is explained in a previous paper on the P22 tailspike protein (Sargent et al., 1988). Further details are given in the original assignments of Lord and co-workers (Chen & Lord, 1974; Lord, 1977) and in recent reviews (Carey, 1982; Spiro, 1987). The prominence of the shoulder at 1653 cm^{-1} in the amide I

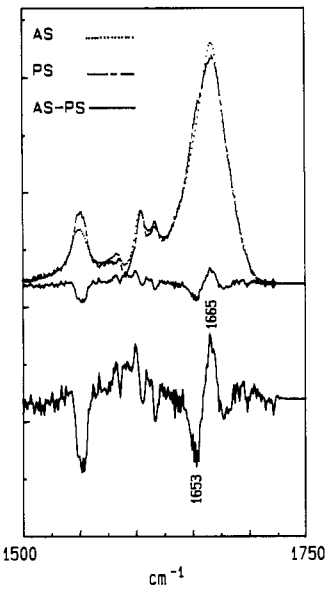

FIGURE 5: Raman spectra of PS (---) and AS (···) in the amide I region, and their difference spectrum, AS minus PS (—). The lowermost trace shows a 4-fold expansion of the difference spectrum, including labels (cm^{-1} units) for the principal amide I difference peaks and troughs.

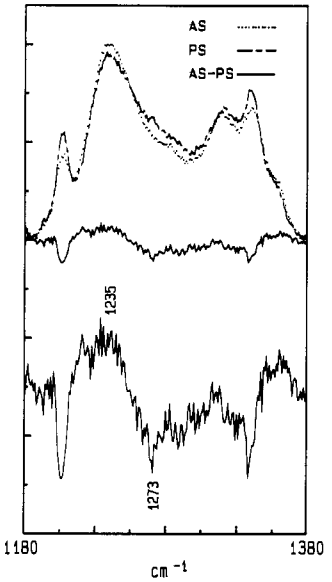

FIGURE 6: Raman spectra of PS (---) and AS (···) in the amide III region, and their difference spectrum, AS minus PS (—). The lowermost trace shows a 4-fold expansion of the difference spectrum, including labels (cm^{-1} units) for the principal amide III difference peaks and troughs.

spectrum of the PS particles and its reduced intensity in the spectrum of the AS particles have been confirmed by Fourier deconvolution (Thomas & Agard, 1984) of the band envelopes (not shown).

We investigated the possibility that the amide I difference shown in Figure 5 might arise from random unfolding of subunits, such as that commonly ascribed to thermal unfolding, but not necessarily a consequence of reconstitution of procapsid shells into associated subunits. We heated the procapsid shells in an attempt to promote thermal unfolding of subunits which could be monitored by Raman spectroscopy. No change in the amide I profile of PS could be detected below 70 °C, and only minimal (≤1%) change could be observed below 80 °C. However, the amide I profile did change significantly at 90 °C. These thermally denatured subunits at 90 °C yielded a Raman amide I profile which was distinctly different from that of AS particles, characterized by a much greater bandwidth and a significantly higher peak frequency, centered at 1671 cm^{-1}. We also repeated these thermal unfolding experiments on AS particles, but found no significant change in the amide I profile at 90 °C. These findings make it unlikely that the subunit structure change profiled in Figure 5, and attendant with the PS → AS transition, is due to a small population of randomly unfolded subunits in the AS preparation.

Also apparent in Figures 5 and 6 are significant changes of Raman intensities at 1207 (Y), 1338 (aliphatic CH_2), and 1552 cm^{-1} (W) associated with vibrations of side chain groups. These are further discussed in a separate section, below.

(b) Quantitative Assessment of the Conformational Switch. The Raman amide I intensity change noted above involves 4.5% (±0.4%) of the total amide I band area, and consists of a 2.2% intensity loss at 1653 cm^{-1} (α-helix) and a 2.3% intensity gain at 1665 cm^{-1} (β-sheet). Identical results were obtained in three separate experimental protocols, including study of shells and subunits from two independent preparations. In measuring the total band area, we integrated over a base line tangent to the minima at 1725 and 1630 cm^{-1} in spectra corrected for the aqueous buffer (Figure 5). The quoted error limit (±0.4%) represents the uncertainty in this base line. By assuming that the same amide I intensity is contributed from each peptide group, we interpret our result to indicate that, on average, 10 ± 1 of the 430 peptide residues of gp5 are converted from α-helix to β-sheet in a conformational switch associated with the PS → AS transition. Validity of the assumption of conservation of amide I intensity among different secondary structures is supported by recent studies of protein crystals (Pezolet & Dousseau, 1990).

The Raman amide III data (Figure 6) are in qualitative agreement with the amide I results, and the respective intensity changes also appear to be quantitatively consistent. We note, however, that Raman amide III intensities are somewhat less predictable than amide I (Lord, 1974), and it would be inappropriate to attempt a computation of quantitative intensity changes in the amide III bands from the data of Figure 6. This would be particularly problematic in the present case because of the overlap of Raman amide III bands of gp5 with additional bands due to tyrosine and aliphatic amino acid side chains, the intensities of which are also clearly affected by the PS → AS transition.

(c) Side Chains Affected by the Conformational Switch. In Figure 7, we show the spectral region 800–890 cm^{-1}, containing bands near 851 and 828 cm^{-1} which are sensitive to hydrogen bonding of phenolic OH groups (Siamwiza et al., 1975) of the eight tyrosines in gp5, and a band near 876 cm^{-1} which is sensitive to hydrogen bonding of indole NH groups (Miura et al., 1988) of the six tryptophans of gp5. The intensity quotient I_{851}/I_{828} falls from 1.57 ± 0.05 in PS to 1.07 ± 0.06 in AS, indicating that AS particles contain more phenolic groups acting as both hydrogen bond donor and hydrogen bond acceptor than is the case for PS. Similarly, the sharp 876 cm^{-1} band in PS is replaced by a broader band at 878 cm^{-1} in AS, indicating a greater distribution of indole NH hydrogen bonding strengths in the latter. Since we see no significant change in the tryptophan 1365 cm^{-1} band (weak shoulder in both PS and AS, cf. Figure 6), we conclude that the tryptophans are not sequestered in hydrophobic environments (Miura et al., 1988) in either PS or AS. All of the observed intensity and frequency shifts in Figure 7 can be explained by hydrogen bonding of more of the tyrosines and more of the tryptophans in AS with solvent H_2O molecules,

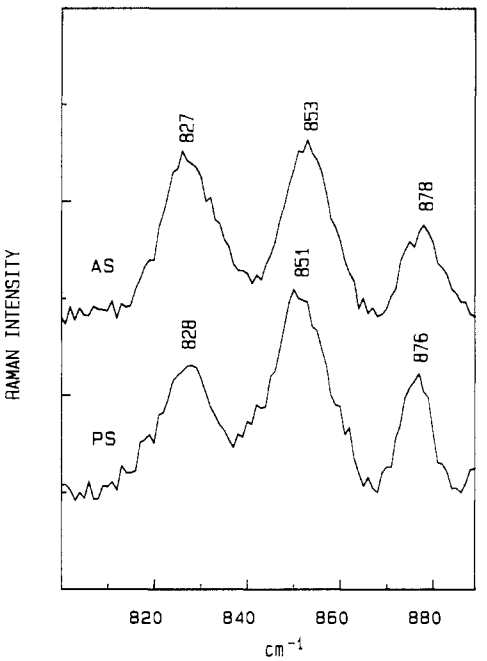

FIGURE 7: Raman spectra of PS (bottom) and AS (top) in the region 800–890 cm^{-1}, showing conformation-sensitive bands of tyrosine and tryptophan side chains. Evident are the increase in half-width and the shift to higher frequency of the tryptophan band of PS at 876 cm^{-1}. Also evident is the substantial decrease in the ratio of intensities of the tyrosine doublet of PS at 851 and 828 cm^{-1}.

i.e., a more solvent-accessible tertiary structure in the AS subunit.

Other spectral changes indicative of different side chain environments in PS and AS occur for bands at 759 (W), 900–960 (aliphatic C–C), 1003 (F), 1125 (A), 1207 (Y), 1338 (aliphatic CH_2), 1400–1450 (aliphatic CH_2 and CH_3), 1552 (W), 1605 (F), and 1618 cm^{-1} (Y). The large relative intensity change of the tryptophan 1552 cm^{-1} band is apparent in Figure 5, and may also reflect altered environments for W residues.

In general, the side chain bands are broader or weaker in AS than in PS particles, consistent with a greater distribution of side chain geometries and/or a greater variety of side chain interactions in the associated subunits than in the subunits of the procapsid shells. These results suggest that the protein monomer in the AS state is typically more exposed to solvent and perhaps less compactly folded than that of the procapsid shell, which is consistent with the polydispersity of AS particles.

Discussion and Conclusions

The assembly of macromolecular structures from protein subunits requires control mechanisms which may be realized through subunit conformational changes. In this paper, we have compared the conformation of P22 coat protein subunits in macromolecular assemblies that are generated by two distinctly different mechanisms. In one, the subunits assemble into well-defined shells utilizing scaffolding protein as a molecular chaperone; in the other, the subunits assemble in the absence of scaffolding protein. Our data indicate that, on average, 4.5 ± 0.4% of the Raman-monitored peptide chain conformational states are affected. This result is reproducible within the quoted limit for independently prepared samples, and for independent runs of the same sample. The data can be explained by a transition of 2.3% or 10 of the 430 residues per gp5 subunit from the α-helix to the β-sheet secondary structure, attendant with the change in assembly mechanism.

It has been shown previously that both in vivo and in vitro in the absence of scaffolding protein that coat protein assembles into three classes of structures: small shells with a radius of 195 Å, large shells with a radius of 262 Å, and spirals with an average length of 1345 Å (Earnshaw et al., 1976). The two shell structures are well-defined. The large shells have a diameter equivalent to that of procapsids and display a surface morphology similar to that of procapsids suggesting a $T = 7$ levo lattice. The small shells also appear very similar to procapsids when visualized by electron microscopy, displaying the serrated surface morphology seen in procapsids. However, the observed X-ray scattering of these particles is best explained by an exterior shell with a $T = 4$ lattice enclosing another shell, perhaps with a $T = 1$ lattice. The spiral structures most likely arise from coat protein in a 6-fold coordinated lattice with 5-fold vertexes inserted at random locations. The spiral structures, while small in number, account for about 40–45% of the total polymerized coat protein subunits.

Our procapsid shells (PS) appear to be the large ($T = 7$) shells. Our associated subunits (AS) are composed by weight of about 50% variously sized shells which are not properly dimensioned procapsid shells (mostly $T = 4$ and $T = 1$) and about 7% monomers, and the remainder existing primarily as spirals. The precise relationship of improperly dimensioned shells in our AS preparations to previously defined shells of gp5 is not clear. However, the electron micrographs reveal a mixture of species, the vast majority of which lack the proper dimensions of the native procapsid.

Closed shells of any diameter and spiral structures cannot arise from aggregation of conformationally random subunits. They represent manifestations of the intrinsic bonding properties of the coat protein subunits.

The associated subunits, which arise from the assembly of biologically active subunits in the absence of scaffolding protein, cannot achieve the conformational requirements fulfilled by the very same subunits in the presence of scaffolding protein. Therefore, we conclude that the conformational difference identified here between subunits of PS and AS particles represents a structural feature mediated most probably by direct interaction between coat protein (gp5) and scaffolding protein (gp8) molecules.

The methods of Raman spectroscopy employed in this work provide structural information averaged over all molecules in the macroscopic sample. For truly homogeneous preparations, such as procapsid shells, the molecular structure detected is the average of the gp5 conformations required to assemble the $T = 7$ particles. On the other hand, since the AS preparations are demonstrably heterogeneous in particle size and shape, it is not possible to relate the observed structural information, and therefore the conformational switch, to a unique type of particle in the ensemble of shells and spirals. The average secondary structure change of 10 residues per polypeptide chain accompanying the PS → AS transition could apply to each subunit in the AS ensemble, or, conversely, the data could be explained by a larger secondary structure change in some smaller fraction of the total associated subunit population. We believe it is important to extend the gp5 association studies to find protocols for isolating monodisperse populations of assembled subunits, including small shells, large shells, and spirals, and submit each of these to further spectroscopic study. Such experiments could provide further insight into the relationships between subunit assembly and specific conformational domains. Future Raman studies of gp5 will also focus on the smaller structural perturbations expected from heat treatment of procapsid shells (J. King, P. E. Prevelige, G. J. Thomas, Jr., and S. A. Towse, unpublished results).

Detailing the conformational switching that accompanies biological assembly is an important problem in developmental biology. We have demonstrated in this paper that Raman spectroscopy can be a sensitive probe of conformational changes affecting macromolecular assembly. Raman spectroscopy would appear to be the method of choice for monitoring conformational switching in these capsid assemblies since particle size and scattering artifacts severely limit the use of other spectroscopic probes, such as NMR and CD spectroscopies.

References

Bazinet, C., & King, J. (1985) *Annu. Rev. Microbiol. 39*, 109–129.

Bazinet, C., Benbaset, J., King, J., Carazo, J., & Carrascosa, J. (1988) *Biochemistry 27*, 1849–1856.

Carey, P. R. (1982) *Biochemical Applications of Raman and Resonance Raman Spectroscopies*, Academic Press, London.

Casjens, S. (1979) *J. Mol. Biol. 131*, 1–13.

Casjens, S., & King, J. (1974) *J. Supramol. Struct. 2*, 202–224.

Caspar, D. L. D. (1980) *Biophys. J. 32*, 103–138.

Caspar, D. L. D., & Klug, A. (1962) *Cold Spring Harbor Symp. Quant. Biol. 27*, 1–24.

Chan, R., & Botstein, D. (1972) *Virology 49*, 257–267.

Chen, M. C., & Lord, R. C. (1974) *J. Am. Chem. Soc. 96*, 4750–4752.

Earnshaw, W., & King, J. (1978) *J. Mol. Biol. 126*, 721–747.

Earnshaw, W., Casjens, S., & Harrison, S. C. (1976) *J. Mol. Biol. 104*, 387–410.

Fuller, M. T., & King, J. (1981) *Virology 112*, 529–547.

Fuller, M. T., & King, J. (1982) *J. Mol. Biol. 156*, 633–665.

Huxley, H. E., & Zubay, G. (1960) *J. Mol. Biol. 2*, 10–18.

King, J., & Casjens, S. (1974) *Nature 251*, 112–119.

King, J., Lenk, E. V., & Botstein, D. (1973) *J. Mol. Biol. 80*, 697–731.

Li, Y., Thomas, G. J., Jr., Fuller, M., & King, J. (1981) *Prog. Clin. Biol. Res. 64*, 271–283.

Lord, R. C. (1977) *Appl. Spectrosc. 31*, 187–194.

Miura, T., Takeuchi, H., & Harada, I. (1988) *Biochemistry 27*, 88–94.

Pezolet, M., & Dousseau, F. (1990) *Biophys. J. 57*, 437a.

Prevelige, P. E., Jr., & Fasman, G. D. (1987) *Biochemistry 26*, 2944–2955.

Prevelige, P., Jr., Thomas, D., & King, J. (1988) *J. Mol. Biol. 202*, 743–757.

Rayment, I., Baker, T. S., Caspar, D. L. D., & Murakomi, W. T. (1982) *Nature 295*, 110–115.

Rossman, M. G. (1984) *Virology 134*, 1–13.

Sargent, D., Benevides, J. M., Yu, M.-H., King, J., & Thomas, G. J., Jr. (1988) *J. Mol. Biol. 199*, 491–502.

Siamwiza, M. N., Lord, R. C., Chen, M. C., Takamatsu, T., Harada, I., Matsuura, H., & Shimanouchi, T. (1975) *Biochemistry 14*, 4870–4876.

Spiro, T. G., Ed. (1987) *Biological Applications of Raman Spectroscopy*, Vol. 1, Wiley Interscience, New York.

Strauss, H., & King, J. (1984) *J. Mol. Biol. 172*, 523–543.

Thomas, G. J., Jr., & Barylski, J. (1970) *Appl. Spectrosc. 24*, 463–464.

Thomas, G. J., Jr., & Agard, D. A. (1984) *Biophys. J. 46*, 763–768.

Thomas, G. J., Jr., Li, Y., Fuller, M. T., & King, J. (1982) *Biochemistry 21*, 3866–3878.

Winston, R., Botstein, D., & Miller, J. (1979) *J. Bacteriol. 137*, 433–439.

^{1}H NMR Studies of Oxidized High-Potential Iron Protein from *Chromatium vinosum*. Nuclear Overhauser Effect Measurements†

J. A. Cowan*,‡ and Marco Sola§

Evans Laboratory of Chemistry, 120 West 18th Avenue, The Ohio State University, Columbus, Ohio 43210, and Department of Chemistry, University of Modena, Via Campi 183, 41100 Modena, Italy

Received December 15, 1989; Revised Manuscript Received February 26, 1990

ABSTRACT: ^{1}H nuclear Overhauser effect experiments on the isotropically shifted signals of oxidized *Chromatium vinosum* HiPIP have been used to identify the four β-CH_2 geminal couples of the cysteine ligands. A partial assignment to individual residues has been proposed from a computer graphics analysis of the X-ray structure. Tentative assignments of other resonances are discussed.

High-potential iron proteins (HiPIP's)[1] are a class of redox proteins containing a $[Fe_4S_4]$ cluster that is bound by four cysteine residues (Carter et al., 1974). HiPIP's have been isolated from a number of bacterial sources and are characterized by unusually high reduction potentials ($E^{\circ\prime} \sim 0.35$ V) that are significantly different from those of related low-potential ferredoxins ($E^{\circ\prime} \sim -0.4$ V), which contain one or two clusters that are structurally identical with the former (Palmer, 1975; Carter, 1977). HiPIP's have been the subject of a variety of spectroscopic studies (Dus et al., 1967, 1973); however, ^{1}H NMR is of particular value for mapping the region around a paramagnetic prosthetic group (Nettesheim et al., 1983; Krishnamoorthi et al., 1986, 1989; Moss et al., 1969; Holm et al., 1974; Que et al., 1974; Reynolds et al.,

† This research was supported by a grant from The Ohio State University.

‡ The Ohio State University.

§ University of Modena.

[1] Abbreviations: HiPIP, high-potential iron protein; NOE, nuclear Overhauser effect; NMR, nuclear magnetic resonance; WEFT, water-eliminated Fourier transform; MODEFT, modified driven equilibrium Fourier transform.

0006-2960/90/0429-5633$02.50/0